ISSN 1028-334X, Doklady Earth Sciences, 2007, Vol. 417A, No. 9, pp. 1380–1385. © Pleiades Publishing, Ltd., 2007.
Original Russian Text © E.F. Sinyakova, V.I. Kosyakov, 2007, published in Doklady Akademii Nauk, 2007, Vol. 417, No. 4, pp. 522–527.

GEOCHEMISTRY

Experimental Modeling of Zoning in Copper–Nickel Sulfide Ores

E. F. Sinyakova and V. I. Kosyakov

Presented by Academician N.V. Sobolev October 29, 2006

Received November 11, 2006

DOI: 10.1134/S1028334X0709019X

The formation of copper–nickel sulfide deposits of the Norilsk and Sudbury types is related to the ore-bearing layered mafic–ultramafic intrusions that are confined to local platform depressions [1–4]. According to the scenario proposed in [5], the initial stages of the deposit formation include the separation of mafic magma into immiscible silicate and sulfide melts, the secondary layering of the sulfide liquid into the fractions enriched in Ni and Cu, and their subsequent gravitational differentiation. The solidification of the Fe–Ni sulfide melt produces pyrrhotite–pentlandite mineralization, while the progressive crystallization of the second fraction leads to the formation of pyrrhotite–pentlandite–chalcopyrite and other ores, including the mineral assemblages with chalcopyrite, bornite, and other minerals. These processes provide the zonal arrangement of ores of different types at the deposits [6] with spatial differentiation of mineral assemblages accompanied by regular variations in contents of both major and trace elements (including PGE) throughout orebodies. For example, the deposits of the Norilsk group demonstrate both simple (pyrrhotite, pyrrhotite–chalcopyrite, and chalcopyrite) and more complex (pyrrhotite, troilite–pyrrhotite–cubanite, cubanite, cubanite–talnakhite, and talnakhite) types of zoning. It is noteworthy that the same differentiation is established in the disseminated ore as well [3, 6].

The spatial differentiation of mineral assemblages is commonly referred to the sequence of their crystallization according to the phase relations in the Cu–Fe–Ni–S system [7], whereas the variation of the chemical composition of minerals in the ore is explained by fractional crystallization [1, 2, 4–6, 8]. Its realization under natural conditions is possible due to nonuniform temperature fields during solidification, diffusive–convective transfer in the solidifying melt, and virtual lack of diffusion of components in solid phases [9]. In the limit case of the conservative system, the melt has a homogeneous composition and equilibrium is established at the melt–crystal interface. As a result, quasi-equilibrium directional crystallization is realized. Thereby, the distribution of phases and components through the volume of a crystalline massif is controlled by the temporal shift in the position of the crystal–melt interface, the initial composition of melt, and the equilibrium partition coefficients of components.

The Rayleigh equation is commonly used in the quantitative description of component fractionation in the process of the quasi-equilibrium directional crystallization of PGE-bearing sulfide melts [1, 4, 8, 10]:

$$x_L = x_{L_0}(1-g)^{k-1}, \quad (1)$$

where x_{L_0} and x_L are concentrations of the component in melt at the onset of the process and in the current moment, g is the fraction of the solidified melt, and k is the interphase partition coefficient that is assumed to be constant.

The inadequacy of the assumption of the constancy of partition coefficients during fractionation of multicomponent melts was pointed out by many authors [1, 4, 8, 11]. This assumption is caused by a deficit of experimental data on variation of these coefficients depending on melt composition and the convenience of using the simplified models of crystallization for the quantitative and occasional semiqualitative analysis. At the same time, the experimental data demonstrate that the assumption k = const is commonly inapplicable to both major components [12] and PGE admixtures [13]. The same conclusion follows from thermodynamic calculations: nonconstancy of partition coefficients of major and minor elements in multicomponent systems is a rule that must be fulfilled even at equilibrium of two ideal solutions. It should be noted that from one to t solid phases can be formed during crystallization of the t-component melt. In the case of multiphase crystalliza-

Institute of Geology and Mineralogy Siberian Branch, Russian Academy of Sciences, pr. akademika Koptyuga 3, Novosibirsk, 630090 Russia; e-mal: efsin@uiggm.nsc.ru

tion, the Rayleigh equation cannot be used even as a rough approximation.

In the general case, it is expedient to use a system of differential equations of quasi-equilibrium directional crystallization [14] for the description of fractionation of components. This system may be applied to an arbitrary dependence of k components on the melt composition during crystallization of one or several phases. For the sake of distinctness, let us write these equations for crystallization of the one-component sample in the four-component system. The variation of concentration of the second to fourth components in the crystal (x_2^S, x_3^S, and x_4^S) and melt (x_2^L, x_3^L, and x_4^L) during crystallization of the one-component sample is described by the following system of equations:

$$\frac{dx_2^L}{d\ln(1-g)} = x_2^L(k_2-1); \quad \frac{dx_3^L}{d\ln(1-g)} = x_3^L(k_3-1); \quad \frac{dx_4^L}{d\ln(1-g)} = x_4^L(k_4-1). \tag{2}$$

The partition coefficients of components $k_2(x_2, x_3, x_4)$, $k_3(x_2, x_3, x_4)$, and $k_4(x_2, x_3, x_4)$ depend on the melt composition.

The pathway of crystallization in the concentration tetrahedron is described by the system of equations

$$\frac{d\ln x_2^L}{d\ln x_4^L} = \frac{k_2-1}{k_4-1}; \quad \frac{d\ln x_3^L}{d\ln x_4^L} = \frac{k_3-1}{k_4-1}. \tag{3}$$

Using the equation from [14], it is easy to describe the crystallization of two- and three-phase samples. The pathway of crystallization consecutively passes through a set of elements of the liquidus surface, and the character of transition from one element to another is determined by the type of phase reaction that accompanies this transition. The moment of transition is accompanied by a break in curves of partition $x_i^S(g)$ of all or separate components in the sample. Quantitative calculations based on the above equations require knowledge of the dependence of partition coefficients on the melt composition, which may be found from experimental data or solution of the equations of phase equilibria for the specified thermodynamic models of phases in the system. Unfortunately, the data necessary for calculations are very limited even for the ternary systems and are virtually absent for four-component systems. As has been shown in [8], the distribution coefficients of metals and PGE in the Fe–Ni–Cu–S system depend on the concentration of sulfur. However, the wide scatter of experimental points indicates that k depends on the concentration of other components as well. Namely, these circumstances make impossible a rigorous description of fractionation in the basic Cu–Ni–Fe–S (PGE) geochemical system.

An extremely great number of experiments is required to establish the aforementioned relationships in multicomponent systems using traditional methods. In our opinion, this problem can be solved by experimental modeling of fractionation of components in multicomponent systems. Indeed, a share of the crystallized melt has been chosen in the aforementioned equations as a coordinate of the process. In this case, the process under consideration is scale-invariant at the accepted assumptions. Precisely this circumstance served as the basis for the application of Eq. (1) to the approximate analysis of fractionation of ore-forming components. The same property of the quasi-equilibrium directional crystallization provides a principal possibility to reproduce in experiments the solidification of massive orebodies and sulfide disseminations in the silicate matrix. The directional crystallization of the samples with approximately natural melt compositions makes it possible to determine the sequence of crystallization of phases from the melt in the course of its solidification, to trace directly the fractionation of all components of the system, and to calculate the quantitative parameters of the process.

In this communication, we exemplify the crystallization of the melt of the following composition (at %): Fe 32.55, Cu 10.70, Ni 5.40, and S 51.00. This composition is close to the natural melt that produced some Cu–Ni sulfide ores [15]. To study specific features of the fractionation of noble metals, we added 0.05 at % of Pt, Pd, Rh, Ru, Ir, Au, and Ag to the above melt. Our method of the experiment for the quasi-equilibrium directional crystallization of multicomponent sulfide melts, investigation of phase and chemical compositions of crystallized samples, and processing of experimental data are described in [12]. The sample was crystallized at a rate of $2.3 \cdot 10^{-8}$ m/s according to the Bridgman technique. The temperature at the bottom of quartz container at the start and end of crystallization was 1046 and 721°C, respectively. An ingot ~70 mm long and 8 mm in diameter (Fig. 1) was sawed into 24 sections perpendicular to the longitudinal axis. The obtained fragments were used for preparation of polished sections, which were studied under an optical microscope and a LEO 1430VP electron scanning microscope equipped with the EDS. The phase composition of samples was determined with a DRON-3 diffractometer (CuK_α radiation), while the chemical compositions of the phases were examined with a Camebax-micro microprobe. The initial segment of the ingot up to $g \sim 0.68$ was a monocrystalline Fe-mss matrix with its exsolution products as a system of elongated inclusions of the tetragonal Fe-rich intermediate solid solution ($Fe_{0.30}Cu_{0.18}Ni_{0.01}S_{0.50}$ at $g = 0.68$). The inclusions are oriented perpendicular to the growth axis (Fig. 1), and their size gradually increases to the ingot end. The high-temperature mss is transformed during cooling into the low-temperature modification with the structure of monoclinic pyrrhotite (mss^m) in the ingot

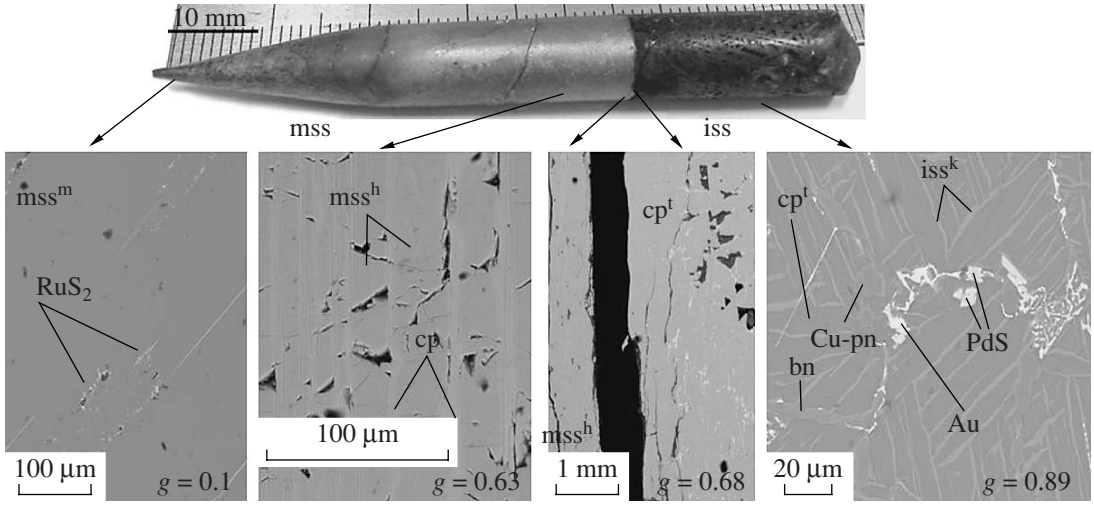

Fig. 1. A sample obtained from directional crystallization (above) and its microstructure (below). Phases of exsolution of the primary mss (left part of the ingot) comprise a monosulfide solid solution with structures of monoclinic (mss^m) and hexagonal (mss^h) pyrrhotite. Phases of exsolution of the primary iss (right part of the ingot) consist of tetragonal chalcopyrite (cp^t), cubic iss (iss^c), Cu-bearing pentlandite (Cu-pn), and bornite (bn). Noble metal minerals are laurite (RuS_2), vysotskite (Pd,Ni)S, and native gold (Au).

segment up to $g = 0.03$ and into mss^h similar to the superstructural hexagonal pyrrhotite (sp. gr. *P*31) in the remaining segment ($g = 0.03$–0.68). The next segment of the ingot was a monocrystalline matrix of the intermediate solid solution (iss). After cooling, the sample was broken along the boundary between these segments. According to the X-ray phase analysis data, the products of the solid-phase iss exsolution comprise tetragonal chalcopyrite $Cu_{0.25}Fe_{0.25}Ni_{0.01}S_{0.49}$ (cp^t) with lamellae of cubic iss (iss^c) and subordinate amounts of pentlandite $Fe_{0.12}Ni_{0.38}Cu_{0.03}S_{0.47}$ and bornite. The melt composition at an arbitrary moment of crystallization was determined from average compositions of the initial mss and iss based on microprobe analysis with an sweeping beam (up to 50 μm in diameter) and equations of mass balance for the components [14]. The partition coefficients of major and minor components were calculated from these data.

The results of the experiments are presented in Tables 1 and 2. The curves of the distribution of major components along the crystallization pathway (Fig. 2) show that the melt is enriched in Cu and depleted in Fe, Ni, and S during the mss crystallization process. The *k* values for Ni and Fe (mss/L) increase with depletion of the melt in S, which is particularly significant for Ni (from 0.9 at the onset of mss crystallization to 1.5 at its end). Thereby, *k* values for Cu and S remain almost constant (0.25 ± 0.03 and 1.05 ± 0.02, respectively). During iss crystallization, Cu and Fe are concentrated in this phase, while the melt is enriched in Ni. At this stage, the *k* value for S is close to unity. At the point of the phase reaction related to the termination of mss crystallization and the beginning of iss crystallization, the pathway of solid phase composition is broken while the pathway of the melt composition is subjected to bending. The transition from one segment to another may be interpreted as a bivariant phase reaction: L + mss → iss.

The estimation of partition coefficients of noble metals is complicated by crystallization of their own phases (Fig. 1). The mss contains laurite RuS_2 inclusions with about 3 at % Ir. The inclusions are concentrated at the very beginning of the ingot. Malanite $CuPt_2S_4$, vysotskite (Pd,Ni)S, silver, and gold with Cu and Pd admixtures are contained in iss. The compositions of laurite, malanite, vysotskite, and native silver were determined with a microprobe (Table 3), and the composition of native gold was estimated on the basis of X-ray spectra of tiny (2–3 μm) grains. It is impossible to determine the composition of other probable phases of noble metals ≤1 μm in size. We managed to estimate the partition coefficients between the mss matrix and melt for Rh, Ru, and Ir (Table 2). The relationships between *k* for Rh and Ru, on the one hand, and the sulfur concentration in the melt, on the other hand, are shown in Fig. 3.

The Cu–Ni ore with the average composition close to the composition of the crystallized melt is characterized by the following mineralogical zoning: monoclinic pyrrhotite–hexagonal pyrrhotite–tetragonal chalcopyrite [6]. According to the phase diagram of the Fe–Ni–Cu–S system [7], pyrrhotite crystallized from the Fe-rich mss during its cooling, whereas chalcopyrite, pentlandite, bornite, and the low-temperature iss are products of the exsolution of high-temperature iss. Hence, the experimental results described above correlate with typical data on the mineralogical structure of sulfide ores. Furthermore, associations of (i) Rh, Ru, and Ir with mss and (ii) Pt, Pd, Au, and Ag with chalcopyrite noted in our experiments are typical of Cu–Ni ores from the Norilsk deposits.

Table 1. Chemical composition of solid phases (mss and iss*)

g	Chemical composition of the solid phase, at %										
	Fe	Ni	Cu	Au	S	Ru	Rh	Pd	Ag	Pt	Ir
0.03	38.56	5.06	2.90	0.00	52.77	0.28	0.18	0.01	0.00	0.00	0.24
0.09	38.76	5.14	3.13	0.00	52.57	0.14	0.15	0.00	0.00	0.00	0.10
0.13	38.20	5.51	3.32	0.00	52.57	0.15	0.14	0.01	0.00	0.00	0.12
0.17	38.32	5.58	3.20	0.00	52.55	0.13	0.13	0.00	0.00	0.00	0.01
0.22	38.10	5.61	3.54	0.00	52.54	0.08	0.08	0.01	0.00	0.00	0.05
0.28	37.86	5.61	3.84	0.00	52.53	0.06	0.06	0.02	0.00	0.00	0.02
0.33	37.72	5.92	3.78	0.00	52.49	0.03	0.05	0.00	0.00	0.00	0.00
0.42	37.14	5.95	4.19	0.01	52.67	0.01	0.03	0.00	0.00	0.00	0.00
0.52	36.72	6.45	4.54	0.00	52.27	0.00	0.00	0.01	0.00	0.00	0.00
0.58	36.45	6.65	4.55	0.01	52.31	0.00	0.00	0.02	0.00	0.00	0.00
0.63	35.96	6.84	4.48	0.02	52.70	0.01	0.00	0.01	0.00	0.00	0.00
0.67	35.75	7.17	4.29	0.02	52.76	0.00	0.00	0.01	0.00	0.00	0.00
0.68*	23.35	3.64	25.25	0.12	47.47	0.00	0.00	0.06	0.06	0.06	0.00
0.72*	23.29	3.18	25.84	0.15	47.30	0.00	0.00	0.09	0.09	0.04	0.00
0.81*	23.68	3.33	25.39	0.14	47.34	0.00	0.00	0.05	0.05	0.03	0.00
0.89*	23.75	2.89	25.89	0.13	47.21	0.00	0.00	0.04	0.09	0.00	0.00
STDEV	0.2–0.3	0.1–0.2	0.3–0.4	0.01	0.1–0.2	0.02–0.03	0.02	0.01			0.04
STDEV*	0.2–0.4	0.4–0.6	0.4–0.6	0.03	0.2–0.4			0.05–0.06	0.02–0.04	0.06	
MDL	0.02	0.02	0.02	0.01	0.02	0.02	0.02	0.02	0.03	0.03	0.03

Note: (STDEV) Standard deviation at the determination of mss and iss compositions with the sweeping microprobe beam; (MDL) microprobe detection limit.

Table 2. Partition coefficients between solid phase (mss and iss*) and melt

g	Fe	Ni	Cu	Au	S	Ru	Rh	Pd	Ag	Pt	Ir
0.03	1.19	0.94	0.26		1.04	6.59	4.06				5.59
0.09	1.21	0.95	0.27		1.03	3.98	3.93				2.33
0.13	1.21	1.02	0.28		1.04	4.72	4.01				3.28
0.17	1.22	1.03	0.26		1.04	4.96	4.27				
0.22	1.24	1.04	0.27		1.04	3.49	2.96				
0.28	1.25	1.04	0.28		1.04	2.93	3.00				
0.33	1.27	1.11	0.27		1.05		2.50				
0.42	1.30	1.13	0.26		1.06						
0.52	1.37	1.29	0.25		1.06						
0.58	1.42	1.39	0.23		1.07						
0.63	1.49	1.52	0.20		1.09						
0.67	1.57	1.72	0.18		1.10						
0.68*	1.03	0.87	1.03	0.80	0.99						
0.72*	1.03	0.87	1.07	1.00	0.99						
0.81*	1.07	0.70	1.07	0.88	0.98						
0.89*	1.12	0.47	1.17	0.76	0.96						

Table 3. Composition of noble metal phases in a sample after directional crystallization and further cooling

g	Phase	Composition, wt % (upper row) and at % (lower row)											Total
		Fe	Ni	Cu	Au	S	Ru	Rh	Pd	Ag	Pt	Ir	
0.03	RuS_2	1.92	0.34	0.39	0.00	37.09	49.65	0.16	0.81	0.00	0.00	9.52	99.88
		1.97	0.33	0.35	0.00	66.00	28.02	0.09	0.44	0.00	0.00	2.83	
0.68	$CuPt_2S_4$	5.06	8.74	14.38	0.00	27.83	0.04	0.00	0.13	0.00	45.64	0.01	101.82
		5.78	9.49	14.42	0.00	55.31	0.02	0.00	0.08	0.00	14.91	0.00	
0.81	(Pd, Ni)S	0.74	6.31	1.51	1.27	23.48	0.03	0.00	67.84	0.00	0.19	0.00	101.37
		0.87	7.07	1.56	0.42	48.12	0.02	0.00	41.89	0.00	0.07	0.00	
1.00	Ag	0.71	0.13	2.19	0.00	0.15	0.03	0.00	0.37	98.00	0.13	0.07	101.78
		1.32	0.23	3.56	0.00	0.47	0.03	0.00	0.36	93.93	0.07	0.04	

It is evident that the laboratory modeling allows only approximate simulation of real processes complicated in nature by a wider compositional range of sulfide magmas (admixtures of Co, As, and others), the presence of refractory oxide particles and gas inclusions, the nonconservative character of the system related to the interaction with fluids, and so on. In addition, the low-temperature transformations (phase transitions, spinodal and binodal breakdown of solid solutions, and subsolidus phase reactions) play a substantial role in natural mineral formation. The influence of metamorphism on the primary mineral assemblages cannot be ruled out as well. Nevertheless, our experiments revealed the most spectacular features of fractionation. The obtained results on the sequence of mineral crystallization and the dependence of partition coefficients of ore components on melt composition may be used for interpretation of mineralogical observations and modeling of solidification of sulfide melts during formation of massive and disseminated Cu–Ni sulfide ores.

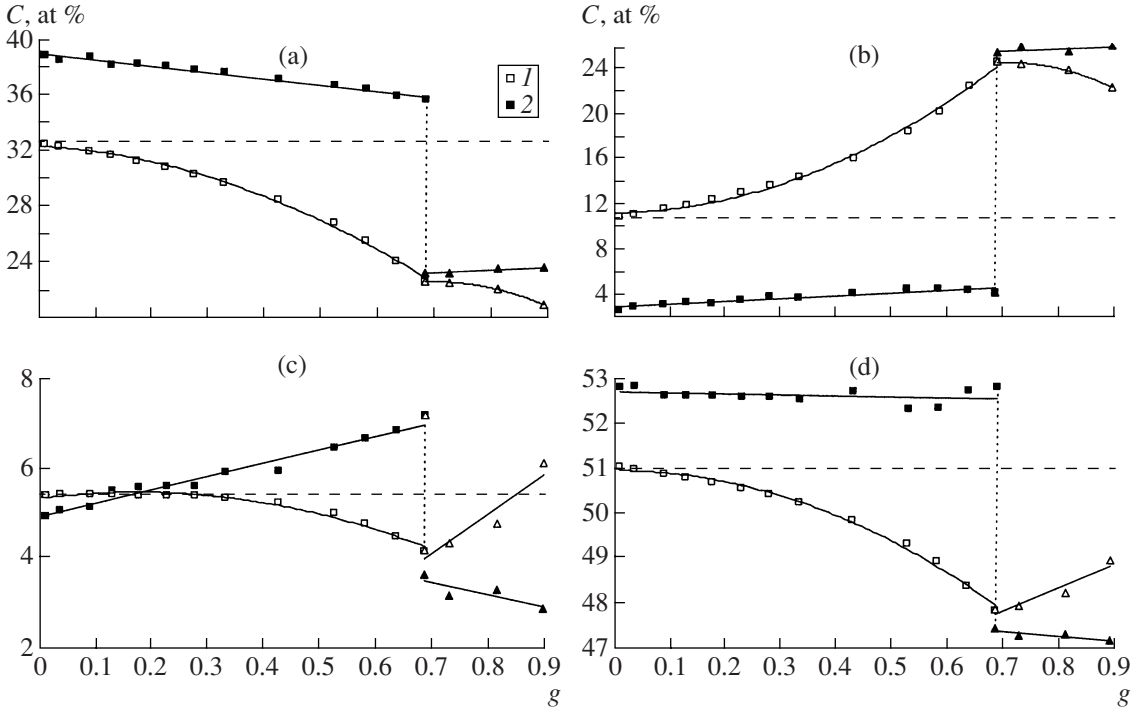

Fig. 2. Distribution of (a) Fe, (b) Cu, (c) Ni, and (d) S in the ingot after directional crystallization of the melt in the (*1*) melt and (*2*) solid phase. The horizontal dashed line is the concentration of the component in the initial melt.

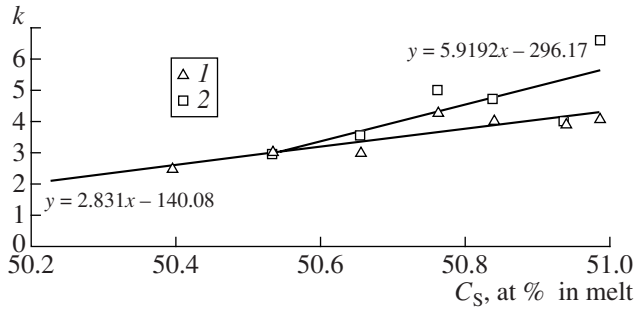

Fig. 3. Partition coefficient of (*1*) Rh and (*2*) Ru vs. S concentration in the melt.

ACKNOWLEDGMENTS

This work was supported by the Russian Foundation for Basic Research, project no. 06-05-64172.

REFERENCES

1. C. Li and A. J. Naldrett, Econ. Geol. **89**, 1599 (1994).
2. N. S. Gorbachev, A. J. Naldrett, V. E. Kunilov, and M. Azif, Dokl. Earth Sci. **371A**, 490 (2000) [Dokl. Akad. Nauk **371**, 362 (2000)].
3. A. A. Marakushev, N. A. Paneyakh, and I. A. Zotov, Petrology **11**, 476 (2003) [Petrologiya **11**, 524 (2003)].
4. D. S. Ebel and A. J. Naldrett, Can. J. Earth Sci. **34**, 352 (1997).
5. A. J. Naldrett, *Magmatic Sulfide Deposits. Geology, Geochemistry, and Exploration* (Springer, Berlin, 2004).
6. V. V. Distler, T. L. Grokhovskaya, T. L. Evstigneeva, et al., *Petrology of Sulfide Magmatic Ore Formation* (Nauka, Moscow, 1988) [in Russian].
7. J. R. Craig and G. Kullerud, Econ. Geol. Monogr. **4**, 344 (1969).
8. S.-J. Barnes, E. Makovicky, M. Makovitsky, et al., Can. J. Earth Sci. **34**, 366 (1997).
9. V. N. Sharapov, A. N. Cherepanov, and V. N. Popov, Geol. Geofiz. **36** (12), 80 (1995).
10. C. Ballhaus, M. Tredoux, and A. Spath, J. Petrol. **42**, 1911 (2001).
11. W. L. McIntire, Geochim. Cosmochim. Acta **27**, 1209 (1963).
12. V. I. Kosyakov and E. F. Sinyakova, Geochem. Int. **43**, 372 (2005) [Geokhimiya **43**, 415 (2005)].
13. E. F. Sinyakova, V. I. Kosyakov, and B. G. Nenashev, Dokl. Earth Sci. **397**, 649 (2004) [Dokl. Akad. Nauk **397**, 670 (2004)].
14. V. I. Kosyakov, Geol. Geofiz. **39**, 1242 (1998).
15. D. S. Ebel and A. J. Naldrett, Econ. Geol. **91**, 607 (1996).